ELSEVIER

Journal of Nuclear Materials 307–311 (2002) 197–202

journal of nuclear materials

www.elsevier.com/locate/jnucmat

Microstructure of irradiated ferritic/martensitic steels in relation to mechanical properties

R. Schaeublin [a,*], D. Gelles [b], M. Victoria [a]

[a] *CRPP-EPFL Fusion Technology Materials, 5232 Villigen PSI, Switzerland*
[b] *Pacific Northwestern National Laboratory, Structural Materials Development, Richland, WA 99352, USA*

Abstract

A review of the microstructure of irradiated reduced activation ferritic/martensitic steels is presented, with a focus on F82H. Because of its resistance to irradiation induced hardening, swelling and low irradiation induced temperature shift in the ductile to brittle transition, this class of steels is a candidate structural material in future fusion reactors. The microstructure induced by irradiation is investigated in order to identify the key elements to deformation mechanisms. The study is focussed on F82H irradiated between 0.5 and 9.2 dpa at temperatures between 250 and 310 °C. Irradiation induced dislocation loops, when resolvable in the TEM, are known to have a Burgers vector $a_0\langle 100\rangle$, while for the smallest visible defects, or 'black spots,' there is still an uncertainty on their type. Black spot damage, possibly due to dislocation loops or precipitates, is investigated. It is attempted to quantitatively relate the dislocation loops and the precipitates to the irradiation induced hardening.

1. Introduction

Martensitic steels provide excellent radiation damage resistance for fission and fusion reactor applications. Significant hardening results from irradiation at temperatures of 400 °C and below, but total elongation remains in the 7% range even in simple Fe–Cr binary alloys [1]. The He production rate for 14 MeV fusion neutrons is 13 appm/dpa, 1 appm/dpa for fission neutrons and about 130 appm/dpa for 590 MeV protons. However, the effect of He on the mechanical properties is believed to be small [2,3] although disagreement exists [4]. H production is about 800 appm/dpa for 590 MeV protons [5] but it is thought that H rapidly escapes the material. However, radiation induced trapping sites may alter H retention. The ferritic/martensitic steels present a good resistance to swelling with a rate of about 1% for 100 dpa [6]. This is understood by the fact that the irradiation induced vacancies are impeded to form voids. The trapping mechanism of the vacancies is still hardly understood, and various models have been proposed [6,7] based on capture by impurities or by dislocations. In the ferritic/martensitic steels irradiation is known to promote a dislocation structure with both $1/2\ a_0\langle 111\rangle$ and $a_0\langle 100\rangle$ Burgers vectors, the latter being predominant when the Cr content is below that of Fe–6Cr [8]. The dislocations with $a_0\langle 100\rangle$ Burgers vector are believed to arise from the growth of irradiation induced faulted $1/2\ a_0\langle 110\rangle$ interstitial loops [7] but more recently an explanation involving $1/2\ a_0\langle 111\rangle$ loop intersections has been proposed [9]. Hardening is understood to arise due to the formation of voids, precipitates, and/or dislocation loops with both $a_0\langle 100\rangle$ and $1/2\ a_0\langle 111\rangle$ Burgers vectors.

This study is focused on the ferritic/martensitic steel F82H, the Japanese candidate material for the future fusion reactor [10]. Irradiation doses are varied from 0.5 to 9.2 dpa, for temperatures ranging from 250 to 330 °C. The lowest doses are intended for the investigation of the early formation of defects, while the highest doses are useful for the study of the evolution of the defect

* Corresponding author. Tel.: + 41-56 310 4082; fax: + 41-56 310 4529.
E-mail address: robin.schaeublin@psi.ch (R. Schaeublin).

0022-3115/02/$ - see front matter
PII: S0022-3115(02)01034-6

structure and the appearance of cavities. It is assumed in the present study that the proton and the neutron irradiations produce the same microstructure, based on a preliminary study [11] and additional confirmation is presented below. While mechanical tests show that, starting at the lowest doses, there is significant hardening induced by irradiation [12], TEM observations of the same material revealed an irradiation induced defect structure that cannot account for the entire hardening. The defect densities and sizes are too low using a dispersed hardening particle model. A discussion of the different possible contributions of the microstructure is presented.

2. Experimental

The F82H ferritic/martensitic steel [10] has a composition of about 7.65 wt% Cr, 2 wt% W, and Mo, Mn, V, Ta, Ti, Si and C below 1 wt% in sum total, and Fe for the balance. The samples were subjected to a heat treatment that gives a fully martensitic structure. It consists of 0.5 h at 1313 K for the normalization, which allows control of the prior-austenite grain size and dissolution of the carbides, and 2 h at 1013 K for tempering.

The proton irradiation was performed in the PIREX (Proton IRradiation EXperiment) facility located in the Paul Scherrer Institut in Villigen, Switzerland, with protons of 590 MeV at three different doses and two different temperatures. The 10 μA proton currents used in the experiments described in the present investigation lead to damage rates of the order of 10^{-7} dpa/s. Temperature is controlled with a thermocouple attached to the sample and He gas at 30 bars which flows through a heater. A full description of the facility and its capabilities is given in Ref. [13]. The neutron irradiations were performed in the HFR at the Netherland Energy Research Foundation ECN located in Petten, Netherlands. The neutrons have an energy spectrum centered around 1 MeV. Temperature control is done by adjustment of the He/Ne gas mixture (respectively higher/lower heat conduction) which cools the sample container. The damage rate deduced from a routine dose of 2 dpa per year is 5×10^{-8} dpa/s. The irradiations presented in this paper were performed with protons from a dose of 0.5–1 dpa at 250 °C and with neutrons from a dose of 2.5–10.3 dpa at temperatures between 250 and 310 °C.

Sample preparation is optimized in order to reduce magnetism and radioactivity by using the following procedure. Samples are punched to produce 1 mm disks, which are then inserted in a 1 mm hole punched into the centers of 3 mm disks of 316 stainless steel. The assembly is then glued with epoxy and mechanically polished to about 100 μm before the usual electropolishing with 10 vol.% perchloric acid, 20% ethylene glycol, 70% methanol at 0 °C and 18 V. Transmission electron microscopy was performed at 200 kV on a JEOL2010 microscope.

3. Results

3.1. The irradiation induced microstructure

Irradiation induced microstructural defects that may induce hardening are interstitials and vacancies, three-dimensional point defect clusters, interstitial and vacancy loops, stacking fault tetrahedra and cavities, namely voids or bubbles filled with gas, in general He. Another type of defects is the irradiation induced precipitation of secondary phase particles. The precipitates that can form by irradiation in the tempered martensite steels are the α' particles, which are coherent bcc Cr rich precipitates, the χ phase particles, which are composed of an intermetallic of Fe and Ni, the σ phase precipitates, which contain Fe and Cr with a tetragonal structure and form between 439 and 828 °C. In addition, carbides already present in the matrix can dissolve and new carbides can form, as $M_{23}C_6$, M_7C_3, M_3C_2 and MC carbides, where M stands mainly for Cr.

Fig. 1(a) presents a weak beam $\mathbf{g}$ ($\sim 4\mathbf{g}$) micrograph obtained with $\mathbf{g} = \{0\,1\,1\}$ showing the irradiation induced damage in F82H irradiated to 1 dpa at 250 ° C. It appears as the so-called black spots, their number density is low compared to fcc materials. In Fig. 1(b) a weak beam $\mathbf{g}$ ($\sim 4\mathbf{g}$) micrograph obtained with $\mathbf{g} = \{0\,1\,1\}$ shows the microstructure induced by 8.8 dpa irradiation in F82H. Irradiation induced loops appear to form a periodic arrangement similar to a square grid with segments oriented along the $\langle 0\,0\,1\rangle$ directions. A denuded zone of about 10 nm near the boundaries is seen in the top of the image. It is indeed observed that regions close to boundaries are depleted of radiation induced structural damage.

Further understanding of the black spot damage was obtained from a series of $\mathbf{g} \cdot \mathbf{b}$ analyses in the case of the 1 dpa and the 8.8 dpa irradiations. Fig. 2 shows weak beam TEM micrographs of F82H irradiated with protons to 1 dpa at 250 °C in the upper images and with neutrons to 8.8 dpa at 302 °C in the lower images. Left images correspond to a weak beam condition $\mathbf{g}$ ($\sim 4\mathbf{g}$) obtained with $\mathbf{g} = \{2\,0\,0\}$ and right images correspond to a weak beam condition $\mathbf{g}$ ($\sim 4\mathbf{g}$) obtained with $\mathbf{g} = \{0\,1\,1\}$. Both conditions are close to a zone axis $\langle 0\,1\,1\rangle$.

The micrographs reveal irradiation induced black spots and dislocation lines at 1 dpa with $\mathbf{g} = \{2\,0\,0\}$ (Fig. 2(a)). As dark field images are shown, black spots appear white on a dark background. The black spots have mean size of 2.4 nm [14] and are homogeneously distributed. A few have a stronger contrast than the others

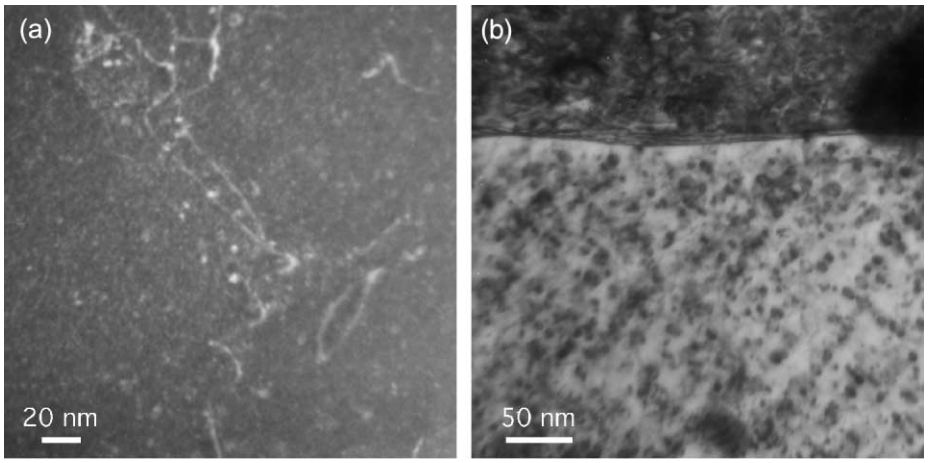

Fig. 1. (a) $\mathbf{g} = (200)$ weak beam TEM image of F82H irradiated in PIREX to 1 dpa at 250 °C and (b) bright field TEM image of F82H irradiated to 8.8 dpa at 302 °C in Petten.

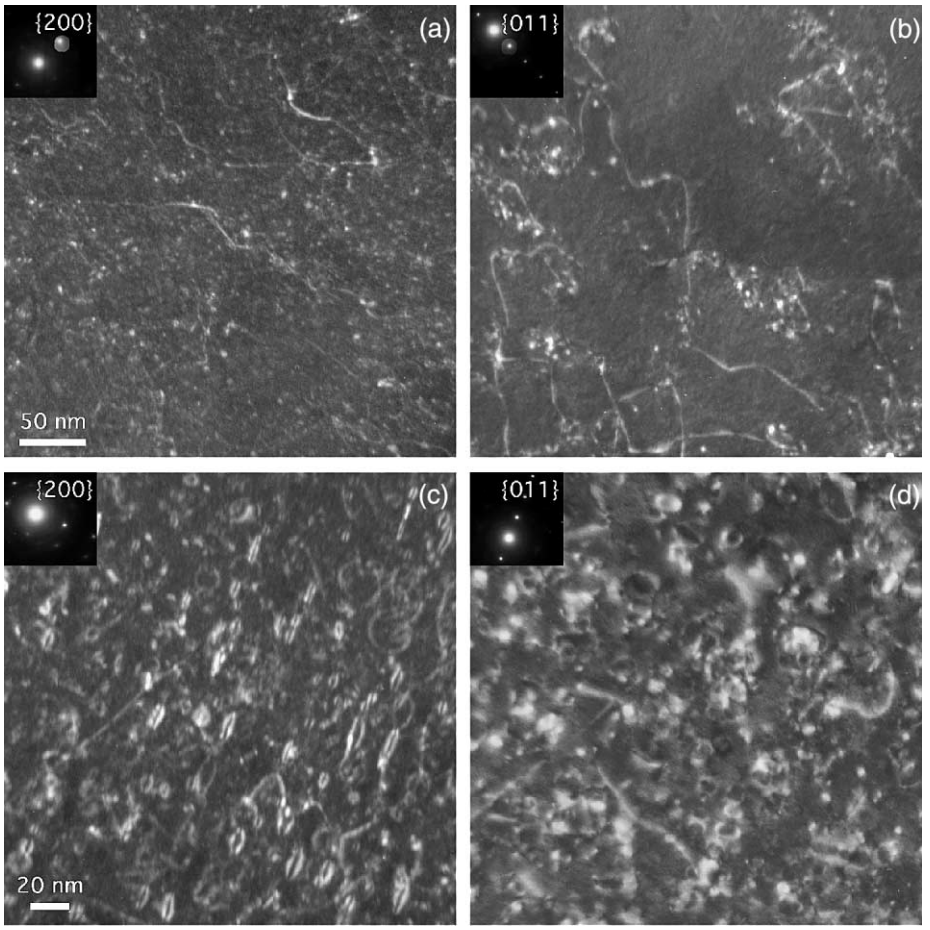

Fig. 2. Weak beam images of F82H irradiated to 1 dpa at 250 °C in PIREX with (a) $\mathbf{g} = \{200\}$ and (b) $\mathbf{g} = \{110\}$ and to 8.8 dpa at 302 °C in Petten with (c) $\mathbf{g} = \{200\}$ and (d) $\mathbf{g} = \{110\}$.

that have contrast intensity similar to the dislocations, which have generally a 1/2 a_0 ⟨1 1 1⟩ Burgers vector [15]. With $\mathbf{g} = \{0\,1\,1\}$ (Fig. 2(b)) less black spots are visible than with $\mathbf{g} = \{2\,0\,0\}$. It was deduced from such an observation that the black spots have a Burgers vector $\mathbf{b} = 1/2\ a_0\ \langle 1\,1\,1\rangle$ ([14], [errata: due to a typographical error in [14] it is wrongly stated that **b** can be and is 1/2 a_0 ⟨1 0 0⟩; it should read that **b** can be a_0 ⟨1 0 0⟩ and is in fact 1/2 a_0 ⟨1 1 1⟩]) for all of them are visible with $\mathbf{g} = \{2\,0\,0\}$ and half of them are visible with $\mathbf{g} = \{0\,1\,1\}$. However, a careful observation indicates that the back spots visible with $\mathbf{g} = \{0\,1\,1\}$ are heterogeneously distributed in the specimen and sit mainly close to dislocation lines. Nearly no black spots are visible far from dislocation lines. It is concluded that the black spots homogeneously distributed and visible with $\mathbf{g} = \{2\,0\,0\}$ in the matrix could be precipitates imaged due to a diffraction spot close to the {2 0 0} matrix spot, because if they were loops having the four possible Burgers vectors $\mathbf{b} = 1/2\ a_0\ \langle 1\,1\,1\rangle$, half of them should be visible with $\mathbf{g} = \{0\,1\,1\}$. In addition, when considering the dislocation decoration in the $\mathbf{g} = \{2\,0\,0\}$ micrograph, it appears that it consists mainly of those black spots that have the strongest contrast. It may be concluded from the $\mathbf{g}\cdot\mathbf{b}$ product magnitude that they have a Burgers vector $\mathbf{b} = a_0\ \langle 1\,0\,0\rangle$, but then two sets of a_0 ⟨1 0 0⟩ loops should still be visible with $\mathbf{g} = \{0\,1\,1\}$.

At 8.8 dpa the microstructure presents irradiation induced dislocation loops that are homogeneously distributed and have a mean size of 5.4 nm. With $\mathbf{g} = \{2\,0\,0\}$ they generally appear edge on, with a strong double dash contrast that is related to a Burgers vector $\mathbf{b} = a_0\ \langle 1\,0\,0\rangle$ (Fig. 2(c)). This is confirmed by molecular dynamics simulations in Fe and TEM image simulation of an interstitial loop sitting on a {1 0 0} plane with a Burgers vector $\mathbf{b} = a_0\ \langle 1\,0\,0\rangle$ [9]. A few loops do not appear edge on and have a Burgers vector $\mathbf{b} = 1/2\ a_0\ \langle 1\,1\,1\rangle$. They appear clearly on Fig. 2(c) as large round loops. With $\mathbf{g} = \{0\,1\,1\}$ it appears that the irradiation induced loops are homogeneously distributed (Fig. 2(d)), contrary to what is observed at low dose (Fig. 2(b)). Note that with $\mathbf{g} = \{2\,0\,0\}$ helical dislocations are observed (Fig. 2(c)) as well as in the case of the low dose.

3.2. Irradiation induced hardening

Mechanical testing showed that the main consequence of irradiation on this class of material is hardening and loss of ductility [12]. We notice first that although, as can be seen in Fig. 2(b), defects clusters decorate dislocations, lengths of dislocations are free of defects. It can be expected then if source hardening is effective no sharp yield drop should be observed. This is actually confirmed by the shape of the tensile curves, which show no such yield point. In order to understand the origin of the radiation hardening in the F82H steel, the disperse obstacle model [16] is used as a basis for the analysis. In this model, the hardening produced by a dispersion of obstacles in the glide plane is described by the relation between the increase of strength induced by the irradiation $\Delta\sigma = \sigma_{\mathrm{irr}} - \sigma_{\mathrm{unirr}}$ and a density of defect clusters N of diameter d according to $\Delta\sigma = \alpha\cdot\mu\cdot b\cdot(Nd)^{1/2}$, where μ is the shear modulus, b the Burgers vector and α is a parameter that describes the strength of the obstacle. For loops and other defect clusters, $\alpha \simeq 0.2$. This model was successfully applied to the case of single crystal Cu and Pd [17,18]. Using the measured strengthening and the observed cluster defect density and mean size in their analysis these authors demonstrated a linear relation between the increase of yield stress and the $(Nd)^{1/2}$, with $\alpha \simeq 0.1$, which corresponds to soft obstacles.

Fig. 3(a) shows first the dependence of the mean obstacle length $(Nd)^{-1/2}$, including data for high doses from irradiations at SINQ, PSI, containing a mixed spectrum of up to 590 MeV protons and neutrons [19]. It indicates that for all types of irradiation particles the

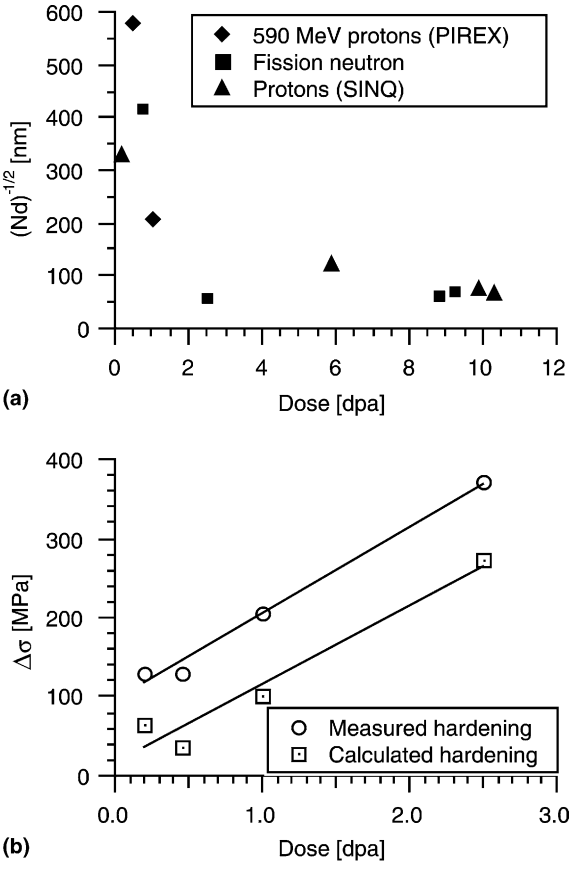

Fig. 3. (a) Dependence of the mean obstacle length $(Nd)^{-1/2}$ with dose and (b) irradiation hardenings, measured and calculated, with their respective linear fit (solid lines).

behavior is comparable: the mean obstacle distance decreases rapidly with dose, saturating at a value of ≃50 nm at approximately 2 dpa. In Fig. 3(b), values of the measured $\Delta\sigma$ together with those resulting from the expression $\alpha \cdot \mu \cdot b \cdot (Nd)^{1/2}$ are plotted versus dose ($\alpha = 1$, corresponding to no particular mechanism, $\mu = 80$ GPa, $b = 0.268$ nm). No values of $\Delta\sigma$ for the SINQ irradiation are yet available, but values of a Fe–12Cr model alloy irradiated with PIREX protons to 0.2 dpa at 250 °C have been added. Two points have to be made: (i) the line for $\Delta\sigma$ does not pass through the origin, having an intersection with the vertical axis at about 100 MPa. This additional hardening has been observed in a number of other polycrystals, as in stainless steel [20] and Ti [21]. Its origin is normally traced to grain size, but it is not really well understood. (ii) The slope of the two linear fits is practically identical. The differences in hardening seem therefore to originate in the difference introduced by a microstructure other than that produced by the irradiation.

4. Discussion

From the observations the following sequence of events could be envisaged to explain the resulting microstructure at high dose:

1. At the beginning of the irradiation the damage consists of small 1/2 a_0 ⟨1 1 1⟩ loops. This is consistent with energetic considerations derived from MD simulations [9] in Fe. These glissile loops have a high diffusivity which explains the lower measured defect density than in the case of irradiated fcc metals.
2. The 1/2 a_0 ⟨1 1 1⟩ loops migrate toward sinks, such as dislocations, where they interact with other 1/2 a_0 ⟨1 1 1⟩ loops to form a_0 ⟨1 0 0⟩ loops according to a reaction of the following type: 1/2 a_0 [1 1 1] + 1/2 a_0 $[1\bar{1}\bar{1}] \rightarrow a_0$ [1 0 0]. The sessile a_0 ⟨1 0 0⟩ loops remain then immobile close to the sinks. The 1/2 a_0 ⟨1 1 1⟩ loops may also interact with the dislocations and produce a local climb that eventually results in helical dislocations.
3. As dose increases the previous reaction propagates from regions close to sinks to regions free of defects for the a_0 ⟨1 0 0⟩ loops become themselves sinks for migrating 1/2 a_0 ⟨1 1 1⟩ loops. In addition, these a_o ⟨1 0 0⟩ loops are stronger sinks to free interstitial than the 1/2 a_0 ⟨1 1 1⟩ loops because of the higher magnitude of the Burgers vector [7]. This is confirmed by a previous analysis of the character of the loops at high irradiation dose concluding that they are predominantly of interstitial type [14]. This leads to the fact that the a_0 ⟨1 0 0⟩ loops tend to grow at the expense of the incoming 1/2 a_0 ⟨1 1 1⟩ loops.
4. At high doses the a_0 ⟨1 0 0⟩ loops dominate the microstructure. The few large 1/2 a_0 ⟨1 1 1⟩ loops that are observed may result from the interaction of moving 1/2 a_0 ⟨1 1 1⟩ dislocations with a_0 ⟨1 0 0⟩ loops according to a scheme of the following type: 1/2 a_0 $[\bar{1}11]$ + a_0 [1 0 0] → 1/2 a_0 [1 1 1] [21].

It appears that the measured hardening is larger than the one calculated using the disperse obstacle model, starting at the lowest doses, by about 100 MPa. One explanation, which applies to other materials (Ti, stainless steel), is that the model does not apply straightforwardly in the case of polycrystals. When considering the detail of the microstructure, it appears that this large increase in hardening can be accounted for by 'black spot damage' that is probably a result of precipitation. The precipitate is not chrome-rich α' because $\mathbf{g} = \langle 0\,1\,1 \rangle$ does not show it. A possibility is MC perhaps due to Ta additions based on observed unexpected hardening in irradiated modified 9Cr–1Mo due to Nb additions [22] but its orientation relationship with the matrix is not yet understood.

5. Conclusion

The evolution of the dislocation loops induced by irradiation in F82H has been rationalized by the formation of small glissile 1/2 a_0 ⟨1 1 1⟩ loops that, with increasing dose, will form sessile a_0 ⟨1 0 0⟩ loops that decorate dislocation lines and eventually fill the whole matrix. Hardening starting at the lowest doses seem to arise, at least partly, from fine precipitation.

Acknowledgements

J.W. Rensman, Petten, is acknowledged for providing the specimens irradiated to the high doses with neutrons. EFDA is thanked for financial support and PSI is acknowledged for the overall use of the facilities.

References

[1] M.L. Hamilton, D.S. Gelles, P.L. Gardner, in: A.S. Kumar, D.S. Gelles, R. Nanstad, E.A. Little (Eds.), Effects of Radiation on Materials: 16th International Symposium, ASTM STP 1175, ASTM, Philadelphia, 1993, p. 545.
[2] K.K. Bae, K. Ehrlich, A. Möslang, J. Nucl. Mater. 191–194 (1992) 905.
[3] K. Shiba, M. Suzuki, A. Hishinuma, J.E. Pawel, in: D.S. Gelles, R.K. Nanstad, A.S. Kumar, E.A. Little (Eds.), Effects of Radiation on Materials: Tenth conference, ASTM STP 1270, ASTM 1996, p. 753.

[4] D. Gelles, J. Nucl. Mater. 283–287 (2000) 838.
[5] S.L. Green, J. Nucl. Mater. 126 (1984) 30.
[6] E.A. Little, J. Nucl. Mater. 87 (1995) 11.
[7] R. Bullough, M.H. Wood, E.A. Little, in: D. Kramer, H.R. Brager, J.S. Perrin (Eds.), Effects of Radiation on Materials: Tenth Conference, ASTM STP 725, ASTM, 1981, p. 593.
[8] D.S. Gelles, J. Nucl. Mater. 108&109 (1982) 515.
[9] J. Marian, B.D. Wirth, R. Schäublin, J.M. Perlado, T. Díaz de la Rubia, these Proceedings.
[10] M. Tamura, H. Hayakawa, M. Tanimura, A. Hishinuma, T. Kondo, J. Nucl. Mater. 141–143 (1986) 1067.
[11] R. Schäublin, M. Victoria, in: S.J. Zinkle, G.E. Lucas, R.C. Ewing, J.S. Williams (Eds.), MRS Symposium Proceedings on Microstructural Processes in Irradiated Materials, vol. 540, 1999, p. 597.
[12] P. Spätig, R. Schäublin, S. Gyger, M. Victoria, J. Nucl. Mater. 258–263 (1998) 1345.
[13] P. Marmy, M. Daum, D. Gavillet, S. Green, W.V. Green, F. Hegedus, S. Proennecke, U. Rohrer, U. Stiefel, M. Victoria, Nucl. Instrum. and Meth. B 47 (1990) 37.
[14] R. Schäublin, M. Victoria, in: G.E. Lucas, L. Snead, M.A. Kirk, Jr., R.G. Elliman (Eds), MRS Symposium Proceedings: Microstructural Processes in Irradiated Materials, vol. 650, 2001, R.1.8.1.
[15] R. Schäublin, P. Spätig, M. Victoria, J. Nucl. Mater. 258–263 (1998) 1178.
[16] A.L. Bement, Proceedings of the Second International Conference on Strength of Metals and Alloys, ASM, Metals Park, OH, 1970, p. 693.
[17] Y. Dai, M. Victoria, in: I.M. Robertson et al. (Eds.), Proceedings of the MRS Symposium on 'Microstructure Evolution during Irradiation' Pittsburg, 1997, p. 319.
[18] N. Baluc, Y. Dai, M. Victoria, in: J.B. Bilde-Sørensen et al. (Eds.), Proceedings of the Twentieth Risø International Symposium on Materials Science on 'Deformation-Induced Microstructures: Analysis and Relation to Properties', Risø National Laboratory, Roskilde, Denmark, 1999, p. 245.
[19] X. Jia, Y. Dai, M. Victoria, J. Nucl. Mater., in press.
[20] C. Bailat, A. Almazouzi, N. Baluc, R. Schäublin, F. Groeschel, M. Victoria, J. Nucl. Mater. 283–287 (2000) 446.
[21] T. Leguey, N. Baluc, R. Schäublin, M. Victoria, J. Nucl. Mater, these Proceedings.
[22] G. Hu, D. Gelles, ASTM STP-956, 1987, p. 83.